A New Splitting Active Contour Framework Based on Chan-Vese Piecewise Smooth Model

LI Can-Fei[1] WANG Yao-Nan[1] LIU Guo-Cai[1]

Abstract On the basis of the Chan-Vese model, a new splitting active contour method for image segmentation is presented. The main idea following is to divide an image into two parts at every iteration, which is similar to the procedure of cell splitting. Then, the model is able to detect all the objects or details in the image. In addition, it enjoys the merit of processing any specific region in the image, even the inconsecutive one. This directly leads to the improvement of computing efficiency whereas segmentation is limited to region of interest (ROI) rather than the whole image. Furthermore, due to the regional constraint of operation, our model outperforms the existing multiphase Chan-Vese model in terms of sensitivity to the initialization. The principle of our model is described in detail, and the method is implemented under the level set framework. Experiments on both synthetic and medical images are carried out, and the comparative results to Chan-Vese model and multiphase Chan-Vese model are also shown.

Key words Image segmentation, deformable model, splitting method, Mumford-Shah model, level set

Since the introduction of the "snake" methodology[1−2] and the proposal of the geodesic active contour model for image segmentation by Caselles et al.[3−4] and Kichenassamy et al.[5], active contours have become particularly popular for segmentation applications[6−9]. These classical snakes and active contour models mainly use an edge-detector, which depends on the gradient of the image to stop the evolving curve on the boundary of the desired object. To make up the shortcomings of edge-detector, Chan and Vese[10] proposed a model based on the Mumford-Shah[11] segmentation technique. With the unnecessity to smooth the initial image, the model can detect objects with very weak boundaries. Besides, it can detect holes in the object. However, the Chan-Vese model has inherent drawbacks. The reason that it can detect holes in the object is that the gray density of the holes is similar to the background. When replaced by other objects whose gray density is close to that of the object, they can not be distinguished from each other (see Fig. 1). In nature, based on the gray densitiy difference, the model divides the image into two parts: one is the background and the other is the object. This means it can only segment images with two regions/classes, but can not segment those with more than two regions/classes. For the latter, multiphase level set[12−15] needs to be used.

Under the basic ideal of dividing one image into two parts, we propose a new splitting active contour model. It is named for the reason that the image is divided into two (one inside curve and one outside curve) at every iteration during the evolution, which is similar to the cell splitting procedure. The model can maintain all the advantages of the Chan-Vese model[11], and is able to break its limitation in segmenting images with more than two classes. In addition, our model is easier to be implemented than traditional multiphase Chan-Vese level set model[12] for it only considers one level set function.

The outline of the paper is as follows. Sections 1 and 2 introduces our model, gives the principle of the model, and formulates the model in terms of level set formulations. The algorithm implementation is described in Section 3. Section 4 includes the validation and image segmentation experiments, and Section 5 is the conclusion.

Received June 26, 2006; in revised form October 31, 2006
Supported by National Natural Science Foundation of China (60375001) and Ph. D. Discipline Special Foundation of China (20030532004)
1. College of Electrical and Information Engineering, Hunan University, Changsha 410082, P. R. China
DOI: 10.3724/SP.J.1004.2008.00659

1 Description of the model

Let the evolving curve C in Ω be the boundary of an open subject ω of Ω (i.e., $\omega \subset \Omega$, and $C = \partial\omega$). The region inside C is represented by ω, and $\Omega\backslash\varpi$ denotes the region outside C.

The basic idea of the model in [10] is as follows. Assume that the image u_n is formed by two approximately piecewise-constant regions with intensities u_n^i and u_n^o. Further, assume that the object to be detected is represented by the region with intensity u_n^i. Let C denote its boundary. Thus, we have $u_0 \approx u_n^o$ outside C, and $u_0 \approx u_n^i$ inside C. Consider an energy function

$$E = F_1(C) + F_2(C) \tag{1}$$

where

$$\begin{aligned} F_1(C) &= \iint_{\Omega_c} |u_0(x,y) - c_1|^2 \mathrm{d}x\mathrm{d}y \\ F_2(C) &= \iint_{\Omega_c} |u_0(x,y) - c_2|^2 \mathrm{d}x\mathrm{d}y \end{aligned} \tag{2}$$

here C is on the boundary of the object, i.e., it is the fittest curve C, the energy function gets the minimum.

$$E_{\min} = \inf(F_1(C) + F_2(C)) \approx 0 \approx F_1(C_t) + F_2(C_t) \tag{3}$$

Obviously,

$$\begin{cases} F_1(C) > 0, F_2(C) \approx 0 & C \text{ outside } O \\ F_1(C) \approx 0, F_2(C) > 0 & C \text{ inside } O \\ F_1(C) > 0, F_2(C) > 0 & C \text{ both inside and outside } O \\ F_1(C) \approx 0, F_2(C) \approx 0 & C \text{ on the boudary of } O \end{cases} \tag{4}$$

See Fig. 1, where O is the object. The energy function gets the minimum only when the curve is on the boundary of the object.

Minimizing the energy function and adding some regularizing terms, Chan and Vese proposed the energy function $F(C, c_1, c_2)$, defined by

$$\begin{aligned} F(C,\ c_1, c_2) = {} & \mu(\text{length}(C) + \nu \cdot \text{are}(\text{inside}(C))+ \\ & \lambda_1 \iint_{\Omega_c} (u_0 - c_1)^2 \mathrm{d}x\mathrm{d}y + \lambda_2 \iint_{\Omega\backslash\Omega_c} (u_0 - c_2)^2 \mathrm{d}x\mathrm{d}y \end{aligned} \tag{5}$$

where μ, ν, λ_1, and λ_2 are fixed parameters, $\mu \geq 0$, $\nu \geq 0$, $\lambda_1 > 0$, and $\lambda_2 > 0$. c_1 and c_2 are the averages inside and outside C, respectively.

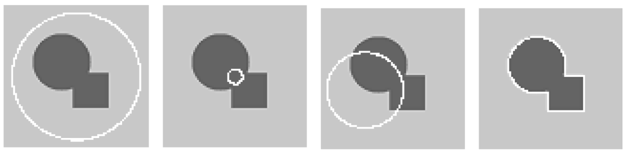

(a) (b) (c) (d)

Fig. 1 Explanation of the basic ideal of the model in [10]

The function acts as dividing an image into two parts in terms of the difference of the average intensity between the background and the object.

Fig. 2 is the segmentation by the model (5). It is shown that the rectangle in the circle cannot be correctly segmented because its gray density is closer to the circle than to the background.

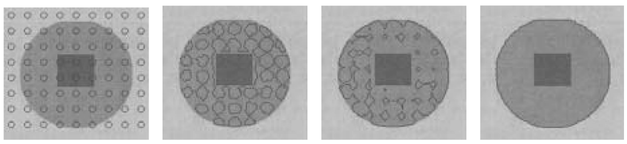

Fig. 2 Result segmented by the model in [10]

To solve the problem, Chan and Vese proposed multiphase level set method[12]. In this paper, motivated by the principle of Chan-Vese model, i.e., splitting an image into two parts in term of the average intensity between the background and the object, we find a different method to solve the previous problem. It finally leads to a new splitting active contour model. Here, we describe our idea as follows.

Let us consider a synthetic image shown in Fig. 3 (a), where a little rectangle is included inside the circle object. Fig. 3 (b) is the segmentation result using the original Chan-Vese model. Here, the curve is the fittest one to divide the image into two parts based on the difference of the average intensity between them. Obviously, the model pulled out the big object only (see Fig. 3 (c)). Further, if we consider a new energy function, and repeat the evolution inside the previous extracted object, we can obtain the segmentation result in Fig. 3 (d), where we have achieve the purpose of segmenting the interior rectangular. Therefore, a new model, the splitting segmentation model comes in focus, and the frame is as follows:

(a) (b) (c) (d)

Fig. 3 Explanation of the basic ideal of our model

$$
\begin{aligned}
&F(C', c_1', c_2') = \mu(\text{length}(C') + \nu \cdot \text{are (inside}(C'))+ \\
&\lambda_1 \iint_{\Omega_c} (u_0' - c_0')^2 \mathrm{d}x\mathrm{d}y + \lambda_2 \iint_{\Omega \backslash \Omega_c} (u_0' - c_2')^2 \mathrm{d}x\mathrm{d}y
\end{aligned} \tag{6}
$$

Obviously, (6) is the same as the model (5) in [10] except for the superscript. This is important to indicate the distinction between our model and the Chan-Vese model in [10]. Similar to (5), where $\mu, \nu, \lambda_1, \lambda_2$ are fixed parameters, $\mu \geq 0$, $\nu \geq 0$, $\lambda_1 > 0$, $\lambda_2 > 0$, and in all our numerical calculations, we fix $\nu = 0$.

For the first splitting stage, u_0' is the initial image to be segmented, $C'$is the evolving front in the image, c_1', c_2' are the averages of u_0' inside and outside C', respectively. After the first splitting, the image is divided into two parts: one is the part inside C' (where $\phi < 0$, and ϕ corresponds to the signed distance functions of level set method described in the following section) and the other is the part outside C' (where $\phi > 0$). Accordingly, there are two parts to be segmented for the second splitting and the segmentation process is similar. To segment the part outside the old curve C', u_0' is the new image pulled out from the old image (where $\phi > 0$), and c_1', c_2' are the averages of the new image inside and outside the new evolving curve C', respectively. This can be implemented conveniently under the level set framework. After the second splitting, we obtain four, i.e., 2^2 parts totally. If necessary, the splitting process can be continued to the nth, and the original images will be divided into 2^n parts mostly. As a post-processing step, all the splitting results are merged to form the final segmentation. For a specific image, the splitting times and the segmentation precision are correlative. The splitting times can be computed according to the precision. Assume that there are M gray levels in an image, then, the precision can be calculated from $m = M/2^n$, where n is the splitting times. Usually, the gray value is from $0 \sim 255$, i.e., $2^8 = 256$ gray levels. Then, at most 8 splitting times are needed to reach single gray level precision. For the resolvable limit of naked human eyes is approximately 20 gray scales, only 4 or 5 splitting times are enough for general applications.

Generally, the basic ideal behind our new model is to divide each region into two parts by splitting during the segmentation (see Fig. 4), which is similar to the cell′s splitting. Therefore, we named it the splitting segmentation model. At first glance, our model seems difficult to implement because of its splitting characteristic. Actually, it is easier than the multiphase level set for the reason that it uses only one level set function but evolves with the same formula. For all the splitting, the algorithm implementation is similar except for a little difference in the first splitting step. This will be explored further in Sections 4 and 5.

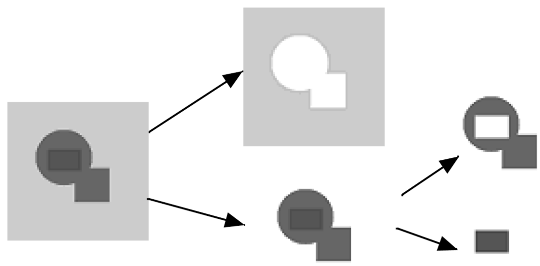

Fig. 4 Ideal of our model, where the splitting is the characteristic

2 Level set formulation of the model

The level set method was originally proposed by Osher and Sethian[16]. It describes the evolving curve implicitly by using the zero level set $\phi(x,y)=0$. Usually the level set function $\phi(x,y)$ is taken as a signed distance function (SDF), i.e., $\phi(x,y)=0$ on the curve, $\phi(x,y)<0$ inside the curve, and $\phi(x,y)>0$ outside the curve. Thus,

$$\begin{cases} C=\partial\omega=\{(x,y)\in\Omega:\phi(x,y)=0\} \\ \text{inside}\,(C)=\omega=\{(x,y)\in\Omega:\phi(x,y)<0\} \\ \text{outside}\,(C)=\Omega\backslash\bar{\omega}=\{(x,y)\in\Omega:\phi(x,y)>0\} \end{cases} \tag{7}$$

In [11], by minimizing $F(C,c_1,c_2)$, the level set formulation of (5) is obtained as

$$\begin{cases} \dfrac{\partial\phi}{\partial t}=\delta(\phi)[\mu\nabla\cdot\dfrac{\Delta\phi}{|\Delta\phi|}-\nu+\lambda_1(u_0-c_1)^2-\lambda_2(u_0-c_2)^2] \\ \phi(0,x,y)=\phi_0(x,y) \quad \text{in } \Omega \\ \dfrac{\delta(\phi)}{|\nabla\phi|}\cdot\dfrac{\partial\phi}{\partial n}=0 \quad \text{on } \partial\Omega \end{cases} \tag{8}$$

where n denotes the exterior normal to the boundary; $\partial\phi$, and $\partial\phi/\partial n$ represents the normal derivative of ϕ at the boundary.

Analogously, by minimizing $F(C',c'_1,c'_2)$, the level set formulation of our model is

$$\begin{cases} \dfrac{\partial\phi'}{\partial t}=\delta(\phi')[\mu\nabla\cdot\dfrac{\Delta\phi'}{|\Delta\phi'|}-\nu+\lambda_1(u'_0-c'_1)^2- \\ \qquad \lambda_2(u'_0-c'_2)^2] \\ \phi'(0,x,y)=\phi'_0(x,y) \quad \text{in} \quad \Omega' \\ \dfrac{\delta(\phi')}{|\nabla\phi'|}\cdot\dfrac{\partial\phi'}{\partial n}=0 \quad \text{on} \quad \partial\Omega' \end{cases} \tag{9}$$

where similar to (8), n denotes the exterior normal to boundary $\partial\phi'$, and $\partial\phi'/\partial n$ denotes the normal derivative of ϕ' at the boundary as before.

3 Numerical approximation of the model

To extend the evolution to all level sets of ϕ', and also to ensure algorithmic stability, $\delta(\phi')$ is replaced by $|\Delta\phi'|$[11]. Then, the level sets formulation is rewritten to

$$\frac{\partial\phi'}{\partial t}=|\Delta\phi'|\,[\mu\nabla\cdot\frac{\Delta\phi'}{|\Delta\phi'|}-\nu+\lambda_1(u'_0-c'_1)^2-\lambda_2(u'_0-c'_2)^2] \tag{10}$$

For $k=\nabla\cdot\frac{\Delta\phi'}{|\Delta\phi'|}$, it can also be described as

$$\frac{\partial\phi'}{\partial t}=\mu k\,|\Delta\phi'|+|\Delta\phi'|\,[-\nu+\lambda_1(u'_0-c'_1)^2-\lambda_2(u'_0-c'_2)^2] \tag{11}$$

Then, ϕ' can be obtained by solving the partial differential equation (11). For the first term is independent of the curvature, the upwind finite difference[17] is used for the discrete case. Because the second term is dependent on the curvature, the central difference[18] is used instead.

Because the level set function does not remain SDF through the evolution, the reinitializing step is necessary as mentioned in [9, 19], to assure that ϕ' does not become too flat or too steep near the curve C'. The reinitialization is implemented by using the following equation[19]:

$$\begin{cases} \dfrac{\partial\phi'}{\partial t}=\text{sgn}(\phi')(1-\|\nabla u'\|) \\ \phi'(0,\cdot)=\phi'(t,\cdot) \end{cases} \tag{12}$$

(12) is a partial differential equation (PDE), which can be discretized using upwind finite differences as above for it is independent of the curvature.

The algorithm is divided into three stages. Stage 1 is the first splitting segmentation, which is the same as the Chan-Vese model. Stage 2 is the subsequent splitting segmentation. Stage 3 is the merger of all the splitting.

Stage 1. Operating on the original image.

1) Give a freely initial curve C', initialize ϕ'_0 by computing the sign distance function, and $n=0$.

2) Compute the averages c'_1, c'_2, inside C' and outside C', respectively.

3) Solve the PDE in ϕ from (11) to obtain ϕ'^{n+1}.

4) Reinitialize ϕ'^{n+1} to the signed distance function by (12) (this step is optional).

5) Check whether the solution is stationary. If not, $n=n+1$ and go to 2) of Stage 1. If yes, $\phi'_0=(\phi'^n>0)$ (to detect the objects outside the curve), or $\phi'_0=(\phi'^n<0)$ (to detect the objects inside the curve), enter Stage 2.

Stage 2. Operating on the new image which is pulled from the original image.

1) $u'_0=I'$. I' is the new image pulled out, which is composed of the pixels, where $\phi'^n>0$ (resp. $\phi'^n<0$) if to detect the objects outside (resp. inside) the curve.

2) Initialize the ϕ'_0 in the new image I' by a new curve C'. Note that the elementary condition in the initialization is to keep ϕ'_0 SDF in the new image I'. In our experiments, we initialized the whole image by using many little circles first, then kept it only in the new image I'. Then we gave a big enough positive or negative constant in the rest area of the old image to make it look as the outer of the new image, which need not be computed (negative or positive depending on the sign of the SDF).

3) After initializing, let $n=0$, and start iteration as 2), 3), and 4) in Stage 1. When the solution is stationary, check whether the segmentation needs to continue. If yes, $\phi'_0=(\phi'^n>0)$ (to detect the objects outside the curve), and $\phi'_0=(\phi'^n<0)$ (to detect the objects inside the curve) and go to 1) of Stage 2. If not, enter Stage 3.

Stage 3. Merge the segmentation results of all the splitting.

4 Experimental results

In this section, we will give some numerical results using our new model on both synthetic and real images. It should be pointed out that the choice of parameters, especially μ, is critical. The μ should take a small value when detecting small objects, and a large value for big ones[11]. In our implementation, the parameter μ is decreased with the iteration times, i.e., a larger value for the first splitting segmentation and smaller ones for the following, which will help to extract useful details. Moreover, since the extracted regions are sparse parts of a matrix, the pixels rested are replaced by 255 in order to show it more clearly.

A synthetic image experiment is shown in Fig. 5. We use the same original image as Fig. 2. It requires twice splitting. The first image is the first splitting result, which corresponds to the result of Fig. 2, and the following images are the second splitting and the final merged segmentation result. In the second splitting, there is only one part that needs to be segmented, where the initialization image, two intermediate results, and the final result are shown. Note that all the objects are detected after the second splitting by using our model.

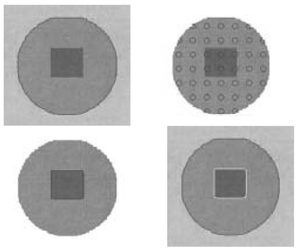

Fig. 5 Example for segmenting synthetic image by the splitting model (The first one is the first spitting result, the following four are in the second splitting course, and the last one is the merged segmentation result.)

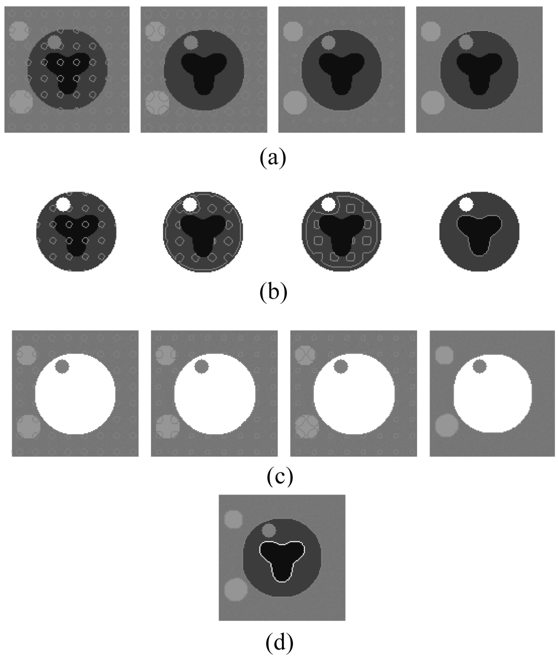

Fig. 6 Example for segmenting synthetic image by the splitting segmentation model ((a) The first splitting segmentation; (b) and (c) The second splitting; (d) The final merged segmentation result)

Another synthetic image experiment is shown in Fig. 6. It needs twice splitting, and both parts in the second splitting need to be segmented. In Fig. 6, (a) is the first splitting, (b) and (c) are the second splitting, (d) is the final merged segmentation result. In Fig. 6 (a), (b), and (c), they are original image or the new image pulled out with the initialization curves, two intermediate results, and the result in the corresponding splitting, respectively. In fact, (a) is the result using the model in [11], which only partitions the image into two parts. The two circles in the background and the star in the middle circle cannot be segmented for their gray density is similar to the gray density of the region around. The interior little circle is correctly segmented because its grey value is close to the background, whereas differs remarkably from those of the round regions. Note that some boundaries segmented in the first splitting are segmented again in the second splitting. Actually, it is the reappearance of the new image boundaries. After the second splitting, all the objects are detected.

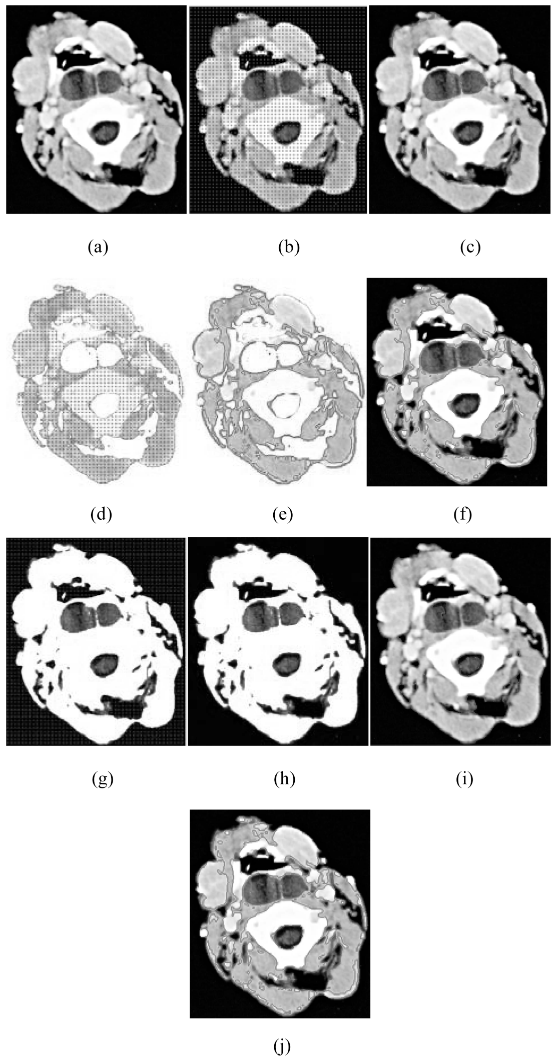

Fig. 7 Segmentation of an MRI by the splitting segmentation model ((a) The original image; (b) The original image with the initialization curves; (d) $\sim$ (f) One part of the second splitting; (g) $\sim$ (i) The other part of the second splitting; (j) The merged segmentation result of the both splitting)

An MRI image segmentation of the splitting segmentation model is shown in Fig. 7. It needs twice splitting. In Fig. 7, (a) is the original image, (b) is the original image with the initialization curves, (c) is the first splitting result, which is also the result using the model in [10], (d), (e), and (f) are one part of the second splitting. Among them, (d) is the new image pulled out from the old image with initialization curves, (e) is the segmentation result shown in the new image, and (f) is the segmentation result shown in the original image. Similarly, (g), (h), and (i) are the other part of the second splitting. The last image (j) is the merged segmentation result of all splitting shown in the original image. In the first splitting, it only segments mainly the contour, and there are many objects not detected. After the second splitting, more objects or more details are detected. If necessary, splitting can be continued to get more objects or details. Generally, the more splitting is made, the more are the objects or details produced. Fig. 8 and Fig. 9 are the segmentation results by multiphase Chan-Vese model[15]. The original image is the same as Fig. 7. Note that their initialization is different. The circles used for the initialization in Fig. 9 are denser than those in Fig. 8. Thus, their segmentation results are different. The two level sets almost overlap together in Fig. 8, but the segmentation in Fig. 9 is similar to the new model.

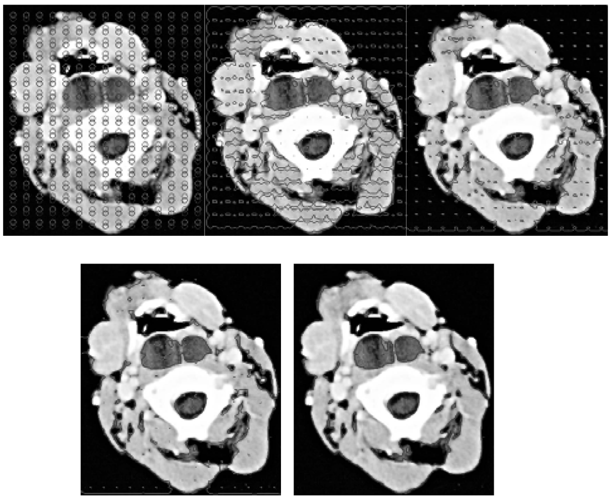

Fig. 8 Segmentation result for an MRI by the multiphase Chan-Vese model in [15]

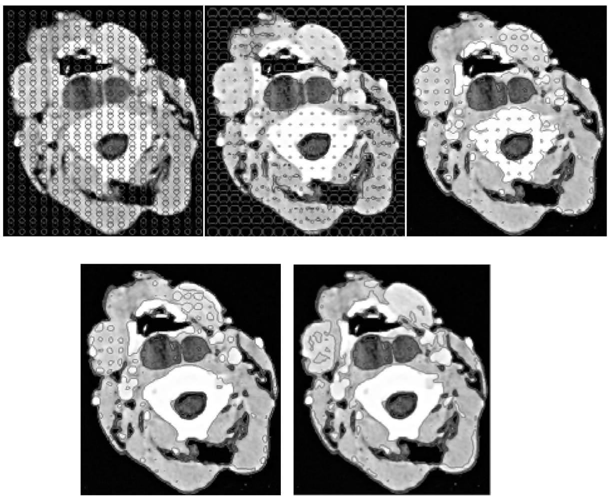

Fig. 9 Segmentation result for an MRI by the multiphase Chan-Vese model in [15]

5 Discussions and conclusion

In this paper, we proposed a splitting active contours model based on the Chan-Vese model and the level set method. Due to the usage of Chan-Vese model in the first splitting, the improved model not only keeps all the original advantages of Chan-Vese model, but also obtained additional merits. First, it can segment all the objects or details in the image if enough splitting is involved in the segmentation process; Second, it is easier to implement than the multiphase level set for it only considers one level set function; Third, the new model is not sensitive to the initialization, for which the multi-phase Chan-Vese model limits the operation only to the pulled out regions in the following splitting; Finally, the data processed in the model can be any regions of an image, even the inconsecutive ones, which leads to the improvement of computing efficiency whereas the segmentation is limited to region of interest (ROI) rather than the whole image. We implemented the model under the level set framework and validated it with both synthetic and real image experiments.

References

1 Kass M, Witkin A, Terzopoulos D. Snakes: active contour models. *International Journal of Computer Vision*, 1988, **1**(4): 321−331

2 Terzopoulos D, Witkin A, Kass M. Constraints on deformable models: recovering 3D shape and nonrigid motion. *Artificial Intelligence*, 1988, **36**(1): 91−123

3 Caselles V, Kimmel R, Sapiro G. Geodesic active contours. In: Proceedings of the 5th International Conference on Computer Vision. Boston, USA: IEEE, 1995. 694−699

4 Caselles V, Kimmel R, Sapiro G. Geodesic active contours. *International Journal of Computer Vision*, 1997, **22**(1): 61−79

5 Kichenassamy S, Kumar A, Olver P, Tannenbaum A, Yezzi A. Gradient flows and geometric active contour models. In: Proceedings of the 5th International Conference on Computer Vision. Boston, USA: IEEE, 1995. 810−815

6 Krissian K, Ellsmere J, Vosburgh K, Kikinis R, Westin C F. Multiscale segmentation of the aorta in 3D ultrasound images. In: Proceedings of the 25th Annual International Conference of the IEEE EMBS. Cancun, Mexico: IEEE, 2003. 638−641

7 Han X, Xu C Y, Prince J L. A topology preserving level set method for geometric deformable models. *IEEE Transactions on Pattern Analysis and Machine Intelligence*, 2003, **25**(6): 755−768

8 Suri J S. Two-dimensional fast magnetic resonance brain segmentation. *IEEE Engineering in Medicine and Biology Magazine*, 2001, **20**(4): 84−95

9 Geomes J, Faugeras O D. Level sets and distance functions. In: Proceedings of the 6th European Conference on Computer Vision-Part I. London, UK: Springer-Verlag, 2000. 588−602

10 Chan T F, Vese L A. Active contours without edges. *IEEE Transactions on Image Processing*, 2001, **10**(2): 266−277

11 Mumford D, Shah J. Optimal approximations by piecewise smooth functions and associated variational problems. *Communications in Pure and Applied Mathematics*, 1989, **42**(4): 577−685

12 Vese L A, Chan T F. A multiphase level set framework for image segmentation using Mumford and Shah model. *International Journal of Computer Vision*, 2002, **50**(3): 271−293

13 Chefd′ Hotel C, Hermosillo G, Faugeras O. A variational approach to multi-model image matching. In: Proceedings of IEEE Workshop on Variational and Level Set Methods in Computer Vision. Vancouver, Canada: IEEE, 2001. 21−28

14 Tsai A, Wells C, Tempany E, Grimson A, Willsky A. Mutual information in coupled multi-shape model for medical image segmentation. *Medical Image Analysis*, 2004, **8**(4): 429−445

15 Chan T F, Vese L A. Image Segmentation Using Level Sets and the Piecewise-constant Mumford-Shah Model. Technical Report 00−14, University of California at Los Angeles, USA, 2000

16 Osher S, Sethian J A. Fronts propagating with curvature-dependent speed: algorithms based on Hamitlton-Jacobi formulations. *Journal of Computational Physics*, 1988, **79**(1): 12−49

17 Sethian J A. An Analysis of Flame Propagation [Ph. D. dissertation], Department of Mathematics, University of California, USA, 1982

18 Sapiro G. *Geometric Partial Differential Equations and Image Analysis*. Cambridge: Cambridge University Press, 2001

19 Sussman M, Smereka P, Osher S. A level set approach for computing solutions to incompressible two-phase flow. *Journal of Computational Physics*, 1994, **114**(1): 146−159

LI Can-Fei Received her bachelor′s and master′s degrees from College of Electrical and Information Engineering, Hunan University, in 2001 and 2005, respectively. She is a Ph. D. candidate in College of Electrical and Information Engineering at Hunan University. Her research interest covers image recognition, computer vision, and medical image processing. Corresponding author of this paper.
E-mail: olivia.c@163.com

WANG Yao-Nan Received his Ph. D. degree from Hunan University. He was a postdoctor researcher at National University of Defense Technology and an Alexander von Humboldt Stiftung. Now he is a professor in College of Electrical and Information Engineering at Hunan University. His research interest covers intelligent control, intelligent image processing, and intelligent robotics.

LIU Guo-Cai Received his master degree from Southeast University. Now he is an associate professor and is a Ph. D. candidate in College of Electrical and Information Engineering at Hunan University. His research interest covers image recognition, computer vision, and medical image processing.